

Three-dimensional modeling and finite element analysis in treatment planning for orthodontic tooth movement

Hussein H. Ammar,^a Peter Ngan,^b Richard J. Crout,^c Victor H. Mucino,^a and Osama M. Mukdadi^d
Morgantown, WV^a

Introduction: The objective of this study was to demonstrate the potential of 3-dimensional modeling and finite element analysis as clinical tools in treatment planning for orthodontic tooth movement. High stresses in bone and miniscrew implants under load can cause fractures and trauma for orthodontic patients, and treatments are typically planned by using clinical experience or simple 2-dimensional radiographs. **Methods:** Anatomically accurate 3-dimensional models reconstructed from cone-beam computed tomography scans were used to simulate the retraction of a single-rooted mandibular canine with a miniscrew placed as skeletal anchorage. Detailed stress distributions in the implant and peri-implant bone were found, in addition to the effect of the orthodontic bracket hook length and the angulation of retraction force on stress response in the periodontal ligament (PDL). **Results:** The numeric results showed that the equivalent von Mises stress on the miniscrew under a 200-cN tangential load reached 42 MPa at the first thread recession, whereas von Mises stress in the peri-implant bone only reached 11 MPa below the neck. High tightening loads of 200 N·mm of torsion and 460 cN of axial compression resulted in much greater bone and implant von Mises stresses than tangential loading, exceeding the yield strengths of the titanium alloy and the cortical bone. Increasing the hook length on the orthodontic bracket effectively reduced the canine PDL stress from 80 kPa with no hook to 22 kPa with a hook 7 mm long. Angulating the force apically downward from 0° to 30° had a less significant effect on the PDL stress profile and initial canine deflection. The results suggest that stresses on miniscrew implants under load are sensitive to changes in diameter. Overtightening a miniscrew after placement might be a more likely cause of fracture failure and bone trauma than application of tangential orthodontic force. The reduction of stress along the PDL as a result of increasing the bracket hook length might account for steadier tooth translation by force application closer to the center of resistance of a single-rooted canine. The relatively minor effect of force angulation on the PDL response suggests that the vertical placement of miniscrews in keratinized or nonkeratinized tissue might not significantly affect orthodontic tooth movement. **Conclusions:** This model can be adapted as a patient-specific clinical orthodontic tool for planning movement of 1 tooth or several teeth. (*Am J Orthod Dentofacial Orthop* 2011;139:e59-e71)

Anchorage is an important consideration for orthodontists and is often an essential component in treatment planning. Of particular clinical

From West Virginia University, Morgantown.

^aGraduate Research Assistant, Department of Mechanical and Aerospace Engineering, College of Engineering and Mineral Resources.

^bProfessor and chair, Department of Orthodontics, College of Dentistry.

^cProfessor, Department of Periodontics, College of Dentistry.

^dAssistant professor, Department of Mechanical and Aerospace Engineering, College of Engineering and Mineral Resources, Center for Cardiovascular and Respiratory Sciences, West Virginia School of Medicine.

The authors report no commercial, proprietary, or financial interest in the products or companies described in this article.

Supported by grants from NIDCR 1R21DE019561 and WV PSCoR.

Reprint requests to: Osama M. Mukdadi, Department of Mechanical and Aerospace Engineering, PO Box 6106, West Virginia University, Morgantown, WV 26506-6106; e-mail, sam.mukdadi@mail.wvu.edu.

Submitted, March 2010; revised and accepted, September 2010.
0889-5406/\$36.00

Copyright © 2011 by the American Association of Orthodontists.
doi:10.1016/j.ajodo.2010.09.020

value is the situation in which absolute anchorage is required for retraction of anterior teeth or protraction of posterior teeth. Such anchorage can be provided extra-orally with headgear or intraorally by using adjacent teeth or dental implants. The advantage of intraoral anchorage is reduced patient compliance for treatment.^{1,2} This is an important factor, considering that 19% of orthodontic visits in 2004 were by children under 12 years of age, and nearly 77% were by minors less than 18.³ Adults can also be averse to the use of headgear for esthetic or professional reasons.

Temporary skeletal anchorage devices such as miniscrew implants have become increasingly popular in orthodontic tooth movement because of their biocompatibility, small size, and placement versatility. **Figure 1** shows the placement of miniscrews between the roots of the mandibular second premolars and first permanent

molars to retract the anterior canines without forward movement of the posterior molars. Miniscrews provide the option of early or immediate loading without a lengthy initial latency period.⁴ Other advantages include placement versatility because of the relatively small diameter of the endosseous body^{1,5} and relatively simple procedures for placement and removal.² The smooth surface and minimal osseointegration reduce torsional resistance.⁶ Miniscrews can be placed between teeth with sufficient bone density and root clearance, giving orthodontists a variety of placement options.⁷ However, interference with the root or periodontal ligament (PDL) can cause significant anchorage loss and mobility or patient trauma.⁸ Heightened stresses in peri-implant bone from orthodontic loading, miniscrew orientation, surrounding bone quality and quantity, or miniscrew design might result in soft-tissue inflammation, microfractures in the bone or implant, or bone resorption.^{8,9} Such failures can compromise anchorage stability and increase the risk of pain or injury. Low stresses in bone at placement can also result in low primary stability of the implant or bone atrophy.¹⁰ High torque might also cause bone damage or miniscrew fracture, requiring corrective surgery.⁸

Currently, the planning of miniscrew placement is limited to the use of clinical judgment in addition to 2-dimensional panoramic radiographs.¹¹ The use of digital radiography can overcome some problems of image distortions resulting from magnification or image noise and reflections, but stress and strain distributions under orthodontic force application cannot be determined.¹¹ Modern medical imaging, modeling, and finite element (FE) analysis solutions can provide powerful tools for optimizing 3-dimensional (3D) morphology from radiographic scans and determining stress and deflection distributions for complex anatomic geometries such as bone. Previous FE studies on miniscrews have used artificial, nonspecific bone-block geometries, finding critical stress areas and the effects of miniscrew length, diameter, and cortical bone thickness on stress response.¹² Motoyoshi et al¹³ performed nonspecific simulations to test the effects of thread pitch and abutment attachment on miniscrew stresses. Pollei et al¹⁴ conducted FE analyses of miniscrews on various commercial implant designs with patient-specific bone geometry, defining a rigidly bonded implant-bone contact for linear simulation. Gracco et al¹⁵ performed nonspecific 2-dimensional FE simulations of a miniscrew with varying lengths and degrees of osseointegration, reporting that stresses decreased with greater osseointegration. Most FE studies focused solely on simulations with either miniscrews¹²⁻¹⁵ or teeth¹⁶⁻¹⁹ from different, isolated models. The objective of this study was to determine the stress profile on the miniscrew implant and peri-



Fig 1. Clinical orthodontic example of canine retraction with miniscrew anchorage attached by elastics to the hook for space closure without forward movement of the posterior molars.

implant bone caused by both a tangential orthodontic force and tightening loads by using 3D modeling and FE analysis. In addition, the effects of orthodontic bracket hook length and force angulation on resulting stress response of the canine PDL were determined. The long-term goal was to determine the potential of 3D modeling and FE analysis in treatment planning for patient-specific tooth movements.

MATERIAL AND METHODS

Figure 2 shows the procedures for 3D modeling and FE analysis in planning for patient-specific tooth movement with a miniscrew. First, a cone-beam computed tomography (CBCT) scan of a patient's maxilla and mandible was acquired in vivo. Images with a square pixel size of 0.41 mm and a total size of 512 pixels per square were used. A total of 128 layered slices were saved in DICOM format with a 21-cm field of view and imported into Mimics software (version 12.1, Materialise, Plymouth, Mich). The voxel size was approximately $0.41 \times 0.41 \times 0.6$ mm with a maximum smoothing error of half of this voxel volume. A global threshold was defined to isolate bone from soft tissues. Then automatic segmentation operations were performed on the morphology to reduce noise and artifacts. The mandibular left canine was isolated with its root for treatment by using local thresholding on the CBCT images. Scaling and Boolean operations were then carried out to model the PDL as a thin enclosure around the root with an average thickness of approximately 0.3 mm. Models were smoothed before the Boolean subtractions to ensure an even fit. One miniscrew implant design was chosen as anchorage for retraction of the mandibular canine

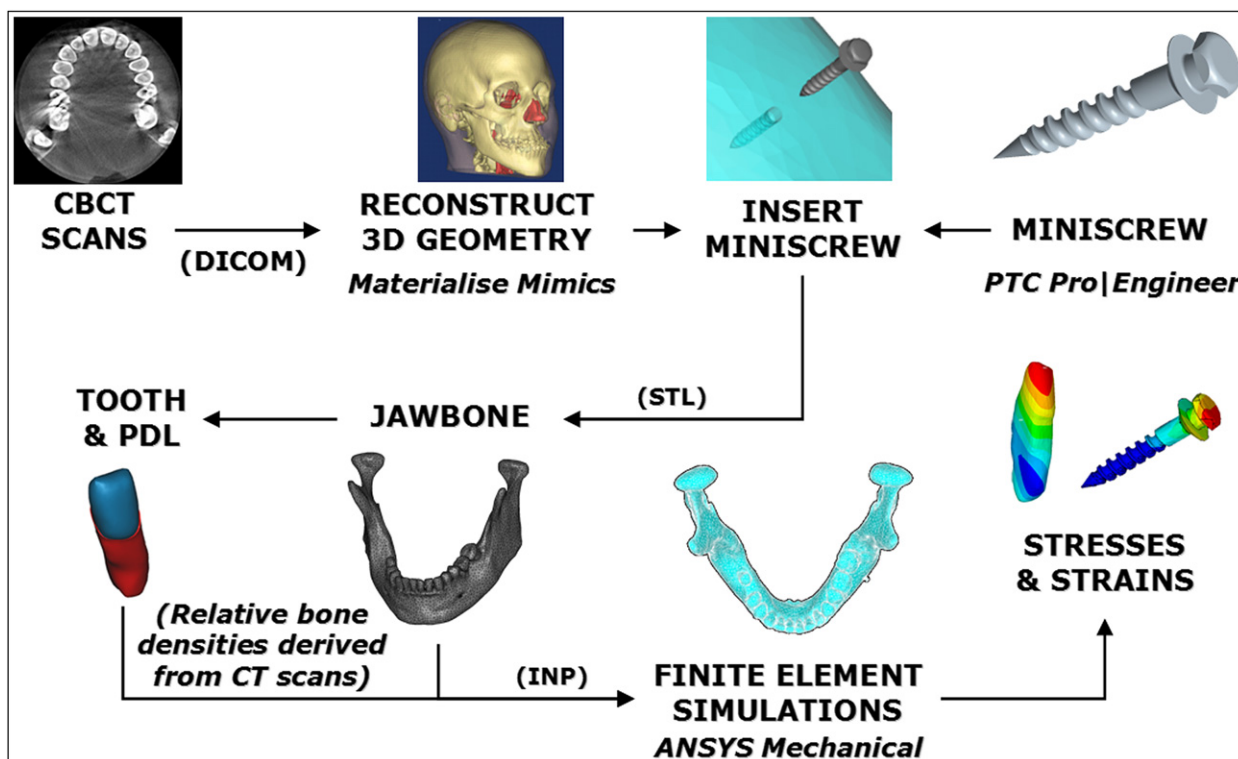


Fig 2. The approach for 3D patient-specific model reconstruction and FE simulation of tooth, PDL, and miniscrew from in-vivo CBCT scans. One patient scan and 1 miniscrew design were studied.

and modeled with the ProEngineer Wildfire software (version 4.0, PTC, Needham, Mass). Dimensions and thread design were based on an implant (ACR OAS-T1207, BioMaterials Korea, La Mirada, Calif) with a thread diameter of 1.2 mm and a total length of 8.7 mm. This implant is constructed from Ti-6Al-4V titanium alloy for biocompatibility and designed for mandibular placement. The model was exported from ProEngineer in stereolithography format into the Mimics software and placed buccally approximately 1.4 cm down from the alveolar ridge between the first and second molars, normally to the cortical surface. Although possibly in unattached mucosa, which increases the risk of inflammation, this location eliminated interference of adjacent roots, and the objective of this study was to analyze detailed miniscrew stress behavior in patient-specific bone.⁸ This allowed us to cut out the bone block around the implant for separate simulation. The cortical layer at this location was also clearly defined in the CBCT images so that patient-specific geometric accuracy would be preserved. A subtraction operation was performed to create a matching drilled hole in the mandibular model. The reconstructed mandible, canine, PDL, and miniscrew were exported into the Mimics-

Table 1. Elastic material properties of anatomic models

Material	Elastic modulus E (GPa)	Poisson's ratio ν	Yield strength (MPa) ²⁵⁻²⁷
Trabecular bone ¹²	1.50	0.30	2
Cortical bone ²⁰	14.7	0.30	133
Tooth ²⁴	20.7	0.30	-
Miniscrew (Ti6Al4V) ²⁷	114	0.34	880
PDL (linear model) ²⁵	6.89×10^{-5}	0.45	-

Remesh module as stereolithography models. A volumetric mesh was then created and optimized by using tetrahedral elements. The optimized meshes of all models including mandible, miniscrew, PDL, and canine were exported from Mimics as ANSYS (version 11.0, ANSYS, Canonsburg, Pa) input files.

The model input files were read into ANSYS as volumetric element meshes by using 4-noded 6-degrees of freedom tetrahedral elements. Model coordinates and positioning of each component into the assembly were also saved. Four contact pairs (Table 1) were created for each of the 4 interfaces: miniscrew-bone, PDL-tooth,

Table II. Contact pair definitions (μ denotes friction coefficient)

Interface	Contact behavior
Miniscrew-bone	$\mu = 0.37^{21}$
PDL-tooth	Bonded
PDL-bone	Bonded
Tooth-bone	$\mu = 0.30^{22}$

PDL-bone, and tooth-bone. The PDL was glued to the canine root and the mandibular socket at the inner and outer surfaces, respectively, to prevent slippage or separation. Contact between the titanium-alloy miniscrew and the mandible was defined with a coefficient of friction equal to 0.37 as the average value reported by Mischler and Pax,²⁰ whereas a coefficient of friction equal to 0.30 was assumed for any possible tooth-bone contact upon excessive PDL compression.²¹

After importing the models into ANSYS, the material properties were defined from literature references (Table II).^{12,19,22-27} All materials used in this study were defined as homogeneous, isotropic, and linearly elastic. Our value for the PDL's elastic modulus was close to correctly documented values from original studies.^{23,27,28} The distribution of bone and tooth elements was determined in the Mimics software by the intensity or gray values of the CBCT scans reported in Hounsfield units (HU). With no loss of generality, the tooth was considered as a homogeneous material. Cortical bone elements were assigned according to an average value of 1400 to 2200 HU, and trabecular bone below 600 HU. These ranges fall within reported HU material limits for CBCT scans.¹⁸ Views of the final FE assembly with individual models and coordinates are shown in Figure 3.

Figure 4 illustrates the simulated load cases of this study. A 200-cN tangential force was applied perpendicular to the miniscrew axis on a central node of the notch in accordance with the reported clinically safe limit for immediate loading.²⁹ A compressive axial force of 460 cN and tightening torque of 200 N·mm were also applied on the miniscrew to simulate maximum placement loading measured experimentally.³⁰ A 100-cN distal horizontal tipping force was applied in 50 load substeps on the buccal crown surface of the canine.³¹ The point of application of the distal force was varied down the long axis of the tooth to simulate the changing hook length. Angulation of the force was varied apically from the occlusal plane to simulate the changing vertical placement of the miniscrew and the angled line of action for an attached spring or elastic band. Nodes at the outer edges of the bone block were fixed to eliminate rigid body motion. Modeling the bone at a distance greater than 4.2

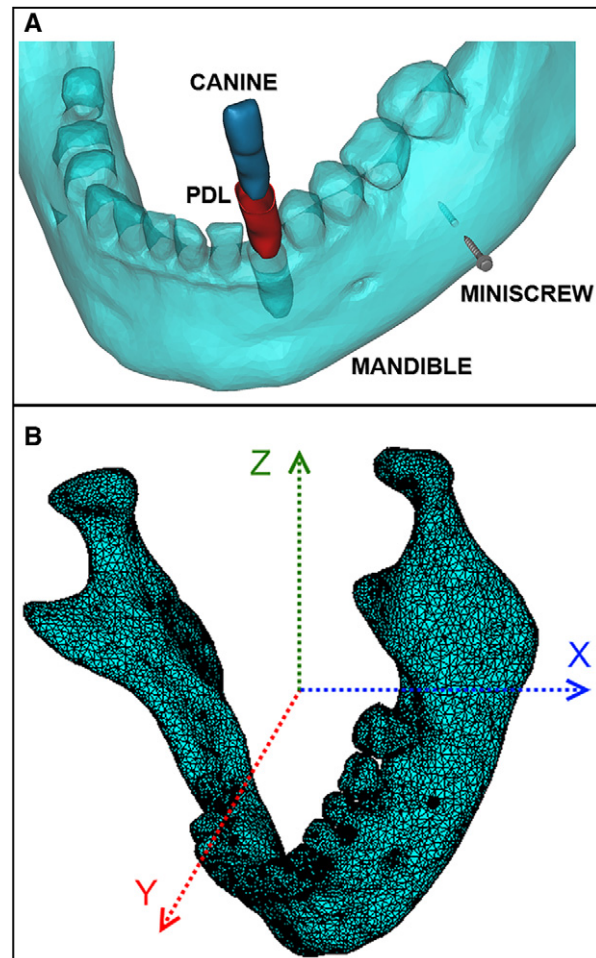


Fig 3. **A**, Three-dimensional views of final patient-specific FE models; **B**, FE mesh with indicated coordinate system ($XY \approx$ occlusal plane, $XZ \approx$ tangential plane, $YZ \approx$ saggital plane).

mm from the site of implant placement yields no significant increase in FE analysis accuracy in the implant region.³² The volumetric meshes of the miniscrew and the surrounding bone were refined near the interface, and stress profile paths were plotted down the length of the miniscrew from neck to tip, down the tooth, and along the inner PDL surface.

RESULTS

Figure 5 shows the equivalent von Mises stress in the miniscrew implant and surrounding bone under a 200-cN tangential force applied at a center node of the miniscrew notch parallel to the cortical bone surface. Implant stresses were plotted along the surface from the neck to the tip, and corresponding von Mises stress distribution

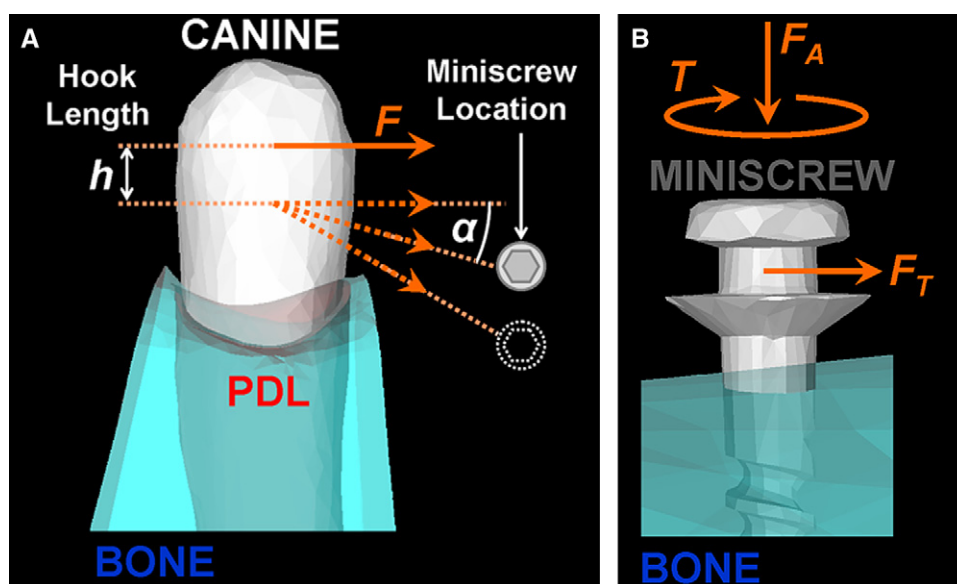


Fig 4. FE loading scenarios for **A**, mandibular left canine subject to distal force F at different vertical hook lengths h and angles α from the occlusal plane corresponding to the changing miniscrew vertical location, and **B**, miniscrew in the bone subjected to orthodontic load (tangential force F_T) and placement loads (tightening torque T and compressive axial force F_A).

contours are shown to the right of each graph. The greatest implant stresses appeared around the neck and at the smallest diameter cross-sections of the upper threads. The tension side of the miniscrew (Fig 5, A) exhibited the highest stress magnitudes, with a maximum von Mises stress of 42 megapascals (MPa) concentrated in the recession of the first thread and steadily decaying farther down the implant. The peri-implant bone experienced considerably lower stresses on the tension side. Little stress appeared in the trabecular bone layer. The compression side of the miniscrew (Fig 5, B) showed lower stress magnitudes and a broader stress distribution. The maximum von Mises stress of 26.5 MPa on the compression side appeared in the first thread. Bone stresses on the compression side were greater than on the tension side, with a distinct peak von Mises stress of 11 MPa above the first bony thread. On the shear side of the miniscrew (Fig 5, C), the local maximum von Mises stresses in the implant can be clearly seen to correspond to the top 6 threads, with the maximum von Mises stress on this path appearing in the second thread recession. Bone stress on this path also showed smoothly decaying behavior.

Relative to the tangential load, the miniscrew experienced much higher stresses under a torque of 200 N·mm and compressive axial force of 460 cN to simulate tightening loads (Fig 6). Maximum von Mises stress in the miniscrew was about 17.3 GPa and appeared in the

second thread (Fig 6, A). Similar to the tangential loading miniscrew stress distribution, maximum von Mises stresses under tightening occurred at the top threads and decayed farther down the screw. The peri-implant bone carried a much lower portion of the total stress under the tightening loads than under the tangential loading, although stress magnitudes were significantly higher under tightening. Maximum bone stress approached 1.4 GPa (Fig 6, B). The twin-peak behavior of the local maximum von Mises stresses in the implant shown in Figure 6, A, corresponds to the implant surfaces oriented at 45°, as shown in the stress profile contour in Figure 6, C. These surfaces correspond to the orientation of the principal planes for maximum compressive or tensile stresses.

In the canine-PDL simulation, a 100-cN distal retraction force was applied at the middle of the buccal crown surface. The displacement distribution plotted in Figure 7 indicated crown-distal tipping and a slight twisting deflection of the canine. Maximum displacement of the tooth under this load was 82.1 μm at the top of the crown. The center of rotation can be seen by qualitative inspection around the top third of the root.

The changes in stress distributions in the PDL with variable bracket hook lengths are shown in Figure 8. The graph was plotted along the inner PDL surface from the distal side to the mesial side with a distal force of 100 cN. The compressive and tensile regions can

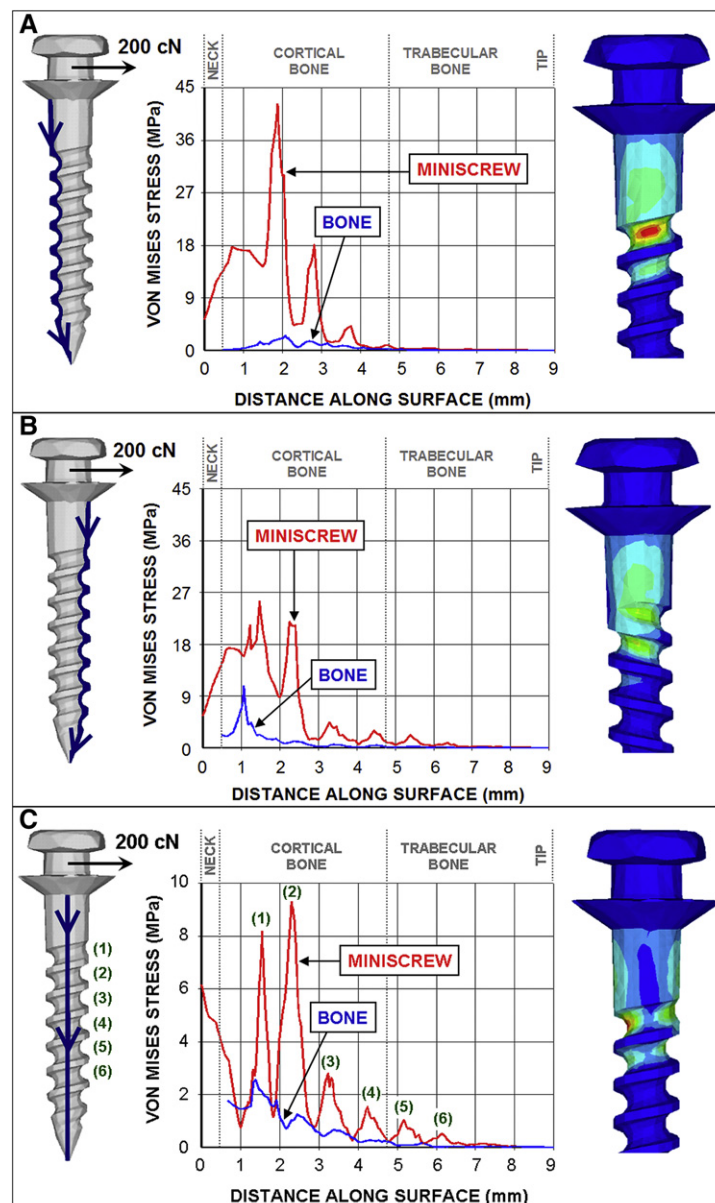


Fig 5. Miniscrew implant von Mises stress under 200-cN tangential force FT plotted down surface of miniscrew from the transmucosal neck to the tip and von Mises contour for **A**, the tension side; **B**, the compression side; and **C**, the shear side.

clearly be seen by the stress curves and correspond to crown-distal tipping, with compressive stresses showing higher magnitudes than tensile stresses. These stresses were much more pronounced than shear stresses. As the hook length (or vertical location of the force application point) was increased from 0 mm at the middle crown surface to 7 mm down the length of the canine, stress magnitudes in the PDL were significantly reduced along most regions. Tensile stress in the mesial PDL

region remained relatively unchanged, although the stress magnitude was slightly reduced and spread over a larger area along the path. Maximum compressive stresses along the distal-mesial inner PDL path decreased from nearly 80 to 22 kPa when the hook length varied from 0 to 7 mm, respectively. Shear stress magnitudes were largely negligible in comparison.

Figure 9 shows the effects of vertical placement of the miniscrew on PDL stresses and deflection of the

canine for a fixed hook length of 2.3 mm. The angle α indicates the angulation of the distal force on the canine from the horizontal occlusal plane downward toward the apex. Maximum compressive and tensile stresses along a distal-mesial path of the inner PDL decreased slightly as the distal force was angled apically downward (Fig 9, A). Shear stresses remained largely unchanged. Deflection of the distal surface of the canine is shown in Figure 9, B, for increasing force angulation. As the force was angled apically downward, canine deflection above the center of resistance (CR) decreased slightly but remained nearly the same below the CR. The location of the canine's CR corresponding to the lowest total deflection also remained steady at nearly two thirds of the root length from the apex.

DISCUSSION

Miniscrew loading

Under a 200-cN tangential force (Fig 5), the miniscrew experienced local maximum von Mises equivalent stresses in each thread recession at the smallest-diameter cross-sections. Similarly, the largest-diameter cross-sections exhibited local minimum stresses. This agrees with previous numeric studies reporting that maximum implant stresses decrease as the endosseus diameter increased.¹² A clinical trial also reported greater success rates for larger screw diameters.²⁹ Another interesting observation was that, although the maximum von Mises stresses appeared in the first or second threads on all sides, rapid decay was observed below the second thread through approximately 2.5 mm of cortical bone. This suggests that the first 2 to 3 mm of this miniscrew implant's endosseus length are the most critical in terms of stress response under tangential loading. In addition, the detailed stress profiles appeared to show little stress in the trabecular bone layer. Previous studies similarly reported maximum stresses near the implant neck and in the upper cortical layer, with lower stresses in trabecular bone.^{12,15}

Yield failure was not predicted in either the miniscrew or the peri-implant bone under the 200-cN tangential load. Maximum von Mises stress in the cortical bone of 10 MPa on the miniscrew's compression side at the top of the first thread was well below the 133-MPa theoretical yield strength of cortical bone, and maximum trabecular bone stress was well below the 2-MPa reported yield strength (Table 1). Similarly, the maximum implant von Mises stress of 42 MPa in the first thread was well below the 880-MPa tensile yield limit of the titanium-alloy miniscrew. These results suggest that this miniscrew design should be able to sufficiently withstand a 200-cN tangential force shortly after loading

through mechanical retention if the patient's bone is healthy. It is also suggested that bone fracture as a direct result of such loading is unlikely if there is no previous damage. Pollei et al¹⁴ speculated that failure in such a case can occur as a result of material fatigue or cycling loads over time. Mastication or disturbance loads caused by the patient might also play a role in possible miniscrew mobility or failure during such a treatment load. Nevertheless, orthodontic miniscrew clinical trials have reported that 200 cN is a safe limit for immediate miniscrew loading, and our results also demonstrated stability.²⁹ Whereas equivalent stresses appearing in the implant are of a similar magnitude to those found in previous FE analysis studies of miniscrews,^{14,15} bone stresses were slightly reduced from previous reports.^{15,33} This might be due to slight variations in cortical bone thickness, miniscrew and bone geometry, or FE analysis simulation boundary conditions and material property definitions.

Stress in the miniscrew under tangential loading was markedly greater on the tension side of bending (Fig 5, A), whereas bone stress was greater on the compression side (Fig 5, B). This can be explained by the implant's top thread on the tension side being pulled from the bone and thus bending fully. On the compression side, however, the bone contact restricts full bending of the implant, and bending stress is instead transferred to the adjacent bone via compression. On the shear side of the miniscrew (Fig 5, C), the local greatest von Mises stresses in the implant clearly corresponded to the top 6 threads, and the maximum von Mises stress on this path appeared in the second thread recession. Bone stress on this path also showed a smoothly decaying behavior and carried a greater proportion of the total equivalent stress, possibly due to the increased shear caused by implant-bone frictional contact.

When the miniscrew implant was subjected to 200 N·mm of tightening torsion and 460 cN of axial compressive force (Fig 6), it experienced much higher stresses relative to the tangential load. The maximum von Mises stress in the miniscrew was about 17.3 GPa in the second thread, well above the 880-MPa yield strength of the titanium-alloy miniscrew. Similar to the tangential loading miniscrew stress distribution, maximum von Mises stresses occurred at the top threads and decayed farther down the screw (Fig 6, A). Maximum bone stress was nearly 1.4 GPa (Fig 6, B), again well above the bone's yield limit, although the bone carried a lower portion of the total stress than in the tangential loading. The stress distribution in each thread was also different than in the tangential loading. The twin-peak behavior of the local

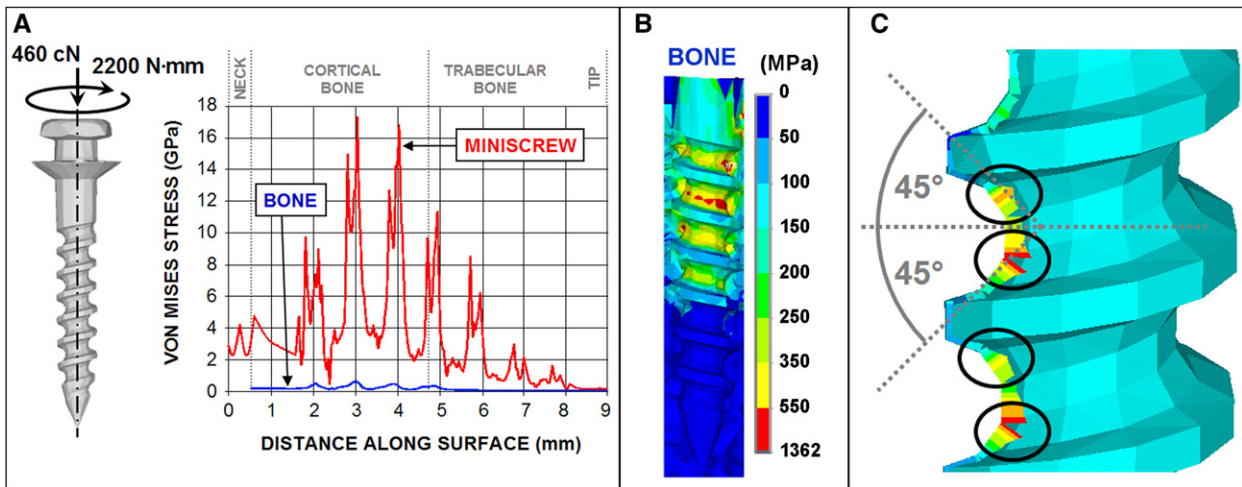


Fig 6. Miniscrew implant von Mises stress under tightening torque T and axial force FA : **A**, plotted down the surface of the miniscrew implant from the transmucosal neck to the tip; **B**, von Mises contour plot of the drilled mandible; and **C**, 45° orientation of the principal planes for maximum stress on the implant surface.

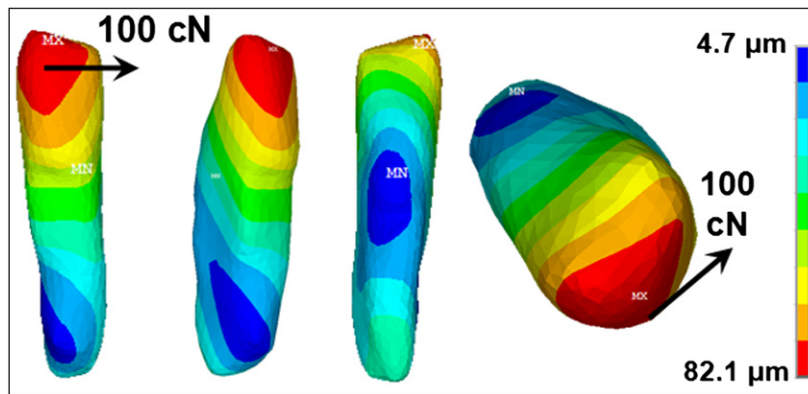


Fig 7. Contour distribution of total deflection (mm) of a canine with linear PDL under crown-distal tipping from the 100-cN horizontal distal load on the buccal crown surface.

maximum von Mises stresses in the implant (Fig 6, A) correspond to the implant surfaces oriented at 45°, as shown in the stress profile contour of Figure 6, C. These surfaces correspond to the orientation of the principal planes for maximum compressive or tensile stresses.

The applied 200 N·mm of torque used in this study was the upper limit measured experimentally by Song et al³⁰ using a similar titanium-alloy miniscrew at the end of the placement process. Thus, rather than actual placement loading, the stress profile under torque and compression in Figure 6 is analogous to the response caused by overtightening the miniscrew shortly after placement, after the bone’s viscoelastic relaxation and

dissipation of residual stresses from drilling. In practice, the astronomically high stress magnitudes of Figure 6 would never be reached; as brittle materials, the miniscrew and bone would fracture at their respective yield points so that postfailure nonlinear analysis is not necessary. Overtightening is a reported clinical risk factor that might cause tissue trauma, microfractures, and loss of anchorage stability.⁹ In addition, excessive torsion has been clinically reported to cause fracture failure of the implant itself.^{2,8} Our results confirm that torsion is a more critical process for miniscrew failure and bone trauma than tangential loading because of the higher stresses generated, as shown quantitatively by the stress profiles. Thus, clinicians should exercise caution

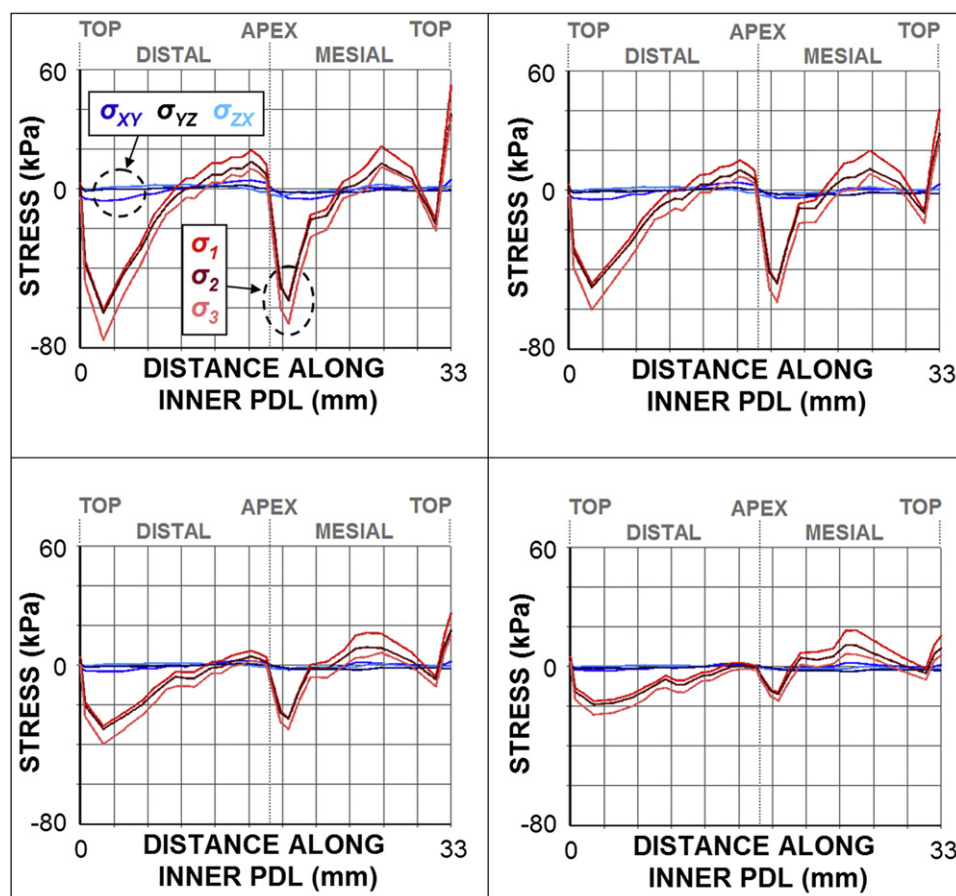


Fig 8. Plots of shear and principal compressive-tensile stress components along the inner PDL from the distal force *F* on the canine applied at the indicated hook lengths *h* from the center of the crown.

during miniscrew placement to prevent exceeding the torque values specified by the implant’s manufacturer. On the other hand, increased miniscrew placement torques have been linked with increased primary stability.³⁴ Motoyoshi et al¹³ recommended placement torque values between 51 and 100 N·mm as an optimal range to ensure primary stability while minimizing the risks of bone damage and miniscrew fracture. Miniscrew manufacturers should expect more failures at the top 2 threads or 2 to 3 mm of a miniscrew’s endosseous length, especially under torsion, and design the miniscrew appropriately, possibly by reinforcing the upper threads or using surface treatments.

Tooth loading

The 100 cN of distal force applied on the simulated canine resulted in distal tipping of the crown (Fig 7) and a slight twisting with a maximum displacement at the crown of 82.1 μm. Modeling the PDL as a nonlinear material resulted in a nearly identical displacement

distribution to that of the linear model in our previous study³⁵; however, the magnitude of displacement was significantly reduced for similar load magnitudes. This difference was likely due to the increasing stiffness of the PDL under increasing loads in experimental tests.³⁶ The relative deflection distribution of Figure 7 is similar to those obtained in previous studies with linear elastic PDLs, although our deflection magnitudes were significantly higher.^{18,19} This might be a result of different model geometries, FE simulation boundary conditions, contact definitions, or variations in the elastic modulus of the PDL. The center of rotation can be identified qualitatively by inspection near the top third of the root, in fair agreement with previous studies.^{19,37}

In this study, we found a reduction of stress magnitudes in the PDL as a result of increasing hook length (Fig 8). This can most likely be attributed to the shorter moment or the power arm from the tooth’s center of rotation to the point of force application, resulting in lower bending stress. Tensile stress in the mesial PDL

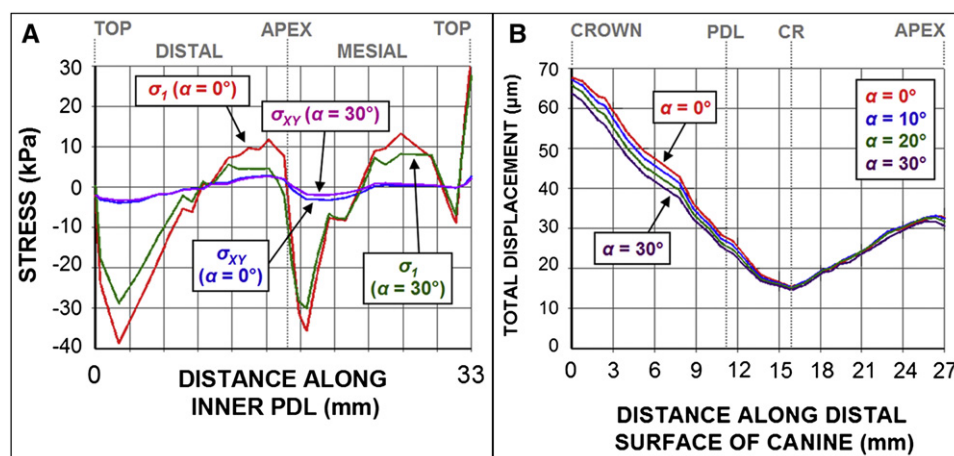


Fig 9. Plots of **A**, first principal and XY shear stresses along the inner PDL, and **B**, total tooth deflection along the distal surface from the distal force F on the canine applied at 0° and 30° from the horizontal occlusal plane (hook length h , 2.3 mm from the crown center).

region remained approximately constant about 20 MPa. Interestingly, compressive stress on the directly opposing distal side decreased. Shear stresses were also noticeably reduced, but compressive and tensile stress components dominated the overall response. High stress magnitudes in the PDL have been associated with ischemia of ligament tissue and abrupt tooth movement³⁷ as well as hyalinization, which might decrease the overall rate of tooth movement by bone necrosis.^{16,38} Excessively high loading states of the PDL are generally considered undesirable in clinical practice, and light forces have been reported by Cattaneo et al¹⁶ as sufficient to cause deformations and mild strains in the PDL. Thus, our results suggest that applying a distal force down the vertical axis of the tooth closer to the CR of the canine can cause steadier, more favorable distal translation from generation of a more uniform PDL stress distribution. Both numeric^{39,40} and in vivo⁴¹ studies have confirmed bodily translation of a tooth in retraction by attaching a power arm or hook and applying a force closer to the CR, granting the orthodontist greater control over tooth movement.⁴²

In our simulation, varying the angulation of the distal force apically downward from the occlusal plane to represent lower buccal placement of the miniscrew resulted in a slight decrease in the first principal stress component as the angle α was increased from 0° to 30° (Fig 9, A), but the effect was relatively subtle compared with the changing hook length. Cattaneo et al¹⁶ reported similar findings using a nonlinear PDL, showing that PDL stress distribution under a 100-cN tipping load was not significantly affected by a vertical mastication force below 500 cN (corresponding to a resultant force

angulation of $\alpha = 79^\circ$). The canine displacement profile (Fig 9, B) showed a slight decrease in displacement for increasing force angulation above the tooth's CR, but again the effect was subtle. The approximate location of the CR at the point of minimum displacement a distance roughly two thirds of the root length from the apex is in fair agreement with previous studies.^{19,37,41} The insignificant effect of the force angle increasing from 0° to 30° on PDL stress and canine deflection suggests that orthodontists have some flexibility on the vertical placement location of a miniscrew in the interradicular space. Brettin et al⁴³ also reported no significant difference in the in-vitro stress response between apical and coronal alveolar-process screw positions. Thus, rather than tooth deflections or stresses in the miniscrew, bone, or PDL, the primary limiting factor in interproximal miniscrew placement might be soft-tissue irritation from placement in unattached or movable mucosa.⁴⁴ Schnelle et al¹¹ suggested flap surgery and the use of a rigid attachment or abutment from the miniscrew head to a more occlusal location, and Motoyoshi et al¹³ reported lower stresses when such an attachment was used. However, the invasiveness and complexity of flap surgery could negate much of the advantage of miniscrew implants in the first place by increasing the risk of postoperative pain⁴⁵ and lengthening the treatment time.¹ Thus, miniscrew placement in attached or keratinized gingiva is clinically favorable, but our results suggest that clinicians have some vertical leeway in this region.

A previous study determined that PDL tensile stress is greater than compressive stress under load.¹⁶ In contrast, stress results in our previous nonlinear PDL study

as well as stress profiles in this linear PDL study (Figs 8 and 9) show that PDL compressive stresses are notably higher than tensile stresses.³⁵ Different FE analysis simulation conditions and contact definitions might account for inconsistencies between numeric studies, indicating lack of standardization. Nevertheless, our results can be interpreted in a general sense. The stress distributions of Figures 8 and 9 largely follow the traditional behavior of linear tipping in terms of tensile and compressive stress regions. Translation behavior and reduced PDL stress became more evident with increasing hook length (Fig 8), whereas increased force angulation or the effective addition of a minor mastication force had little effect on PDL stress and only slightly decreased the tooth's deflection above the CR (Fig 9). These results suggest that hook length or the vertical location at which a distal force is applied has a greater effect on PDL stress distribution (and ensuing tooth movement) than slight force angulation.

Our model used miniscrew to retract a single-rooted mandibular canine. In reality, most orthodontic tooth movement involves several teeth that are connected with wires, and moments and forces are applied to the teeth. We chose a case with the retraction of a single-rooted canine pitted against a miniscrew only as a starting point to demonstrate the efficacy of this new technology. This model can be generalized to include movement of several teeth connected with wires and elastics, by using techniques demonstrated in recent studies along with our unique patient-specific approach.^{39,46} It is expected that 50% of orthodontists will acquire a CBCT machine in their office in the next 5 to 10 years. The use of CBCT technology might soon be the standard of care for orthodontic treatment planning.

Another limitation of this study, and of all orthodontic FE analysis simulation routines, is the inability to directly predict long-term tooth movement quantitatively through simulation. Until the physiologic and biomechanical processes of orthodontic tooth movement are fully understood and represented mathematically in a patient-specific model, this aspect must still be left up to the common clinical practice of experienced orthodontists. In addition, the wide range of boundary conditions, contact definitions, and material property definitions used in current FE analyses creates a genuine need for consistency. Future work should focus on developing a strict set of modeling and simulation standards so that investigators can directly compare their results. Ongoing research is directed toward validation of our preoperative protocol by using in-vivo patient treatment trials in the orthodontic clinic.

CONCLUSIONS

CBCT reconstruction and FE simulation can provide reliable information on the stress pattern around the miniscrew implant and the PDL of the loaded tooth.

1. In our model, the critical areas of stress in the loaded miniscrew were at the top 2 threads in the upper 2.5 mm of cortical bone. Stress response was shown to be sensitive to implant diameter, since local stress peaks appeared in the smallest-diameter sections.
2. Tightening loads caused much greater stress in the miniscrew and peri-implant bone than the tangential force, so the clinician should be careful when tightening the implant to prevent fracture and bone damage.
3. Applying a horizontal retraction force closer to a canine's CR by using a hook reduces stress in the PDL and might account for steadier distal translation of the tooth.
4. Increasing the hook length had a greater effect on the PDL's stress response than angulating the force apically downward, suggesting that vertical placement of miniscrews in keratinized or nonkeratinized tissue might not significantly affect tooth movement.

By using our fully 3D, patient-specific approach, multi-tooth orthodontic systems can be modeled. Moreover, multiple miniscrew placement points can be virtually tested preoperatively to determine the optimal treatment plan. Interference with roots can be predicted, and patient-specific cortical bone thicknesses are preserved. This study demonstrates the potential of our method as an effective clinical tool for optimizing miniscrew anchorage stability and minimizing patient risk.

We thank Materialise for its invaluable technical software assistance and for providing a Mimics project file from the internal database upon request.

REFERENCES

1. Prabhu J, Cousley RRJ. Current products and practice: bone anchorage devices in orthodontics. *J Orthod* 2006;33:288-307.
2. Papadopoulos MA, Tarawneh F. The use of miniscrew implants for temporary skeletal anchorage in orthodontics: a comprehensive review. *Oral Surg Oral Med Oral Pathol Oral Radiol Endod* 2007;103:E6-15.
3. Guay AH, Brown LJ, Wall T. Orthodontic dental patients and expenditures—2004. *Am J Orthod Dentofacial Orthop* 2008;134:337-43.
4. Melsen B, Costa A. Immediate loading of implants used for orthodontic anchorage. *Clin Orthod Res* 2000;3:23-8.

5. Costa A, Pasta G, Bergamaschi G. Intraoral hard and soft tissue depths for temporary anchorage devices. *Semin Orthod* 2005;11:10-5.
6. Mah J, Bergstrand F. Temporary anchorage devices: a status report. *J Clin Orthod* 2005;39:132-6.
7. Poggio PM, Incorvati C, Velo S, Carano A. "Safe zones": a guide for miniscrew positioning in the maxillary and mandibular arch. *Angle Orthod* 2006;76:191-7.
8. Kravitz ND, Kusnoto B. Risks and complications of orthodontic miniscrews. *Am J Orthod Dentofacial Orthop* 2007;131(4 Suppl):S43-51.
9. Wawrzinek C, Sommer T, Fischer-Brandies H. Microdamage in cortical bone due to the overtightening of orthodontic microscrews. *J Orofac Orthop* 2008;69:121-34.
10. Vaillancourt H, Pilliar RM, McCammond D. Finite element analysis of crestal bone loss around porous-coated dental implants. *J Appl Biomater* 1995;6:267-82.
11. Schnelle MA, Beck FM, Jaynes RM, Huja SS. A radiographic evaluation of the availability of bone for placement of miniscrews. *Angle Orthod* 2004;74:832-7.
12. Lim JW, Kim WS, Kim IK, Son CY, Byun HI. Three dimensional finite element method for stress distribution on the length and diameter of orthodontic miniscrew and cortical bone thickness. *Korean J Orthod* 2003;33:11-20.
13. Motoyoshi M, Yano S, Tsuruoka T, Shimizu N. Biomechanical effect of abutment on stability of orthodontic mini-implant. *Clin Oral Implants Res* 2005;16:480-5.
14. Pollei JK, Rocha EP, Ko CC. Stress comparison between orthodontic miniscrews using finite element analysis. *Metro Toronto Convention Centre Exhibit Hall D-E*; 2008.
15. Gracco A, Cirignaco A, Cozzani M, Boccaccio A, Pappalettere C, Vitale G. Numerical/experimental analysis of the stress field around miniscrews for orthodontic anchorage. *Eur J Orthod* 2009;31:12-20.
16. Cattaneo PM, Dalstra M, Melsen B. Strains in periodontal ligament and alveolar bone associated with orthodontic tooth movement analyzed by finite element. *Orthod Craniofac Res* 2009;12:120-8.
17. Cattaneo PM, Dalstra M, Melsen B. The finite element method: a tool to study orthodontic tooth movement. *J Dent Res* 2005;84:428-33.
18. Danielyte J, Gaidys R. Numerical simulation of tooth mobility using nonlinear model of the periodontal ligament. *Mechanika* 2008;71:20-6.
19. Field C, Ichim I, Swain MV, Chan E, Darendeliler MA, Li W, et al. Mechanical responses to orthodontic loading: a 3-dimensional finite element multi-tooth model. *Am J Orthod Dentofacial Orthop* 2009;135:174-81.
20. Mischler S, Pax G. Tribological behavior of titanium sliding against bone. *Eur Cells Mater* 2002;3:28-9.
21. Janssen D, Mann KA, Verdonshot N. Micro-mechanical modeling of the cement-bone interface: the effect of friction, morphology and material properties on the micromechanical response. *J Biomech* 2008;41:3158-63.
22. Lei Z, Feng D, Yi Z, Yubo F. Three dimensional finite element analysis of the initial tooth displacement in different micro implant-bone interfaces using micro-implant anchorage system. *Proceedings of the IEEE/ICME International Conference on Complex Medical Engineering*, 2007;1901-4.
23. Yettram AL, Wright KW, Houston WJ. Centre of rotation of a maxillary central incisor under orthodontic loading. *Br J Orthod* 1977;4:23-7.
24. Black J, Hastings G. *Handbook of biomaterial properties*. London, UK; Springer; 1998.
25. Collings EW. *Materials properties handbook: titanium alloys*. Materials Park, OH: ASM International; 1995.
26. Boccaccio A, Lamberti L, Pappalettere C, Carano A, Cozzani M. Mechanical behavior of an osteotomized mandible with distraction orthodontic devices. *J Biomech* 2006;39:2907-18.
27. Rees JS, Jacobsen PH. Elastic modulus of the periodontal ligament. *Biomaterials* 1997;18:995-9.
28. Ruse ND. Propagation of erroneous data for the modulus of elasticity of periodontal ligament and gutta percha in FEM/FEA papers: a story of broken links. *Dent Mater* 2008;24:1717-9.
29. Crismani AG, Bertl MH, Celar AG, Bantleon HP, Burstone CJ. Miniscrews in orthodontic treatment: review and analysis of published clinical trials. *Am J Orthod Dentofacial Orthop* 2010;137:108-13.
30. Song Y, Cha J, Hwang C. Mechanical characteristics of various orthodontic mini-screws in relation to artificial cortical bone thickness. *Angle Orthod* 2007;77:979-85.
31. Ren Y, Maltha JC, Kuijpers-Jagtman AM. Optimum force magnitude for orthodontic tooth movement: a systematic literature review. *Angle Orthod* 2003;73:86-92.
32. Teixeira ER, Sato Y, Akagawa Y, Shindoi N. A comparative evaluation of mandibular finite element models with different lengths and elements for implant biomechanics. *J Oral Rehabil* 1998;25:299-303.
33. Motoyoshi M, Inaba M, Ono A, Ueno S, Shimizu N. The effect of cortical bone thickness on the stability of orthodontic mini-implants and on the stress distribution in surrounding bone. *Int J Oral Maxillofac Surg* 2009;38:13-8.
34. Wilmes B, Ottenstreuer S, Su YY, Drescher D. Impact of implant design on primary stability of orthodontic mini-implants. *J Orofac Orthop* 2008;69:42-50.
35. Ammar H, Ngan P, Crout R, Mukdadi O, Mucino V. Patient-specific 3D finite-element analysis of miniscrew implants during orthodontic treatment. *Proceedings of the ASME International Mechanical Engineering Congress and Exposition (IMECE)*, 2009; Lake Buena Vista, FL.
36. Toms SR, Lemons JE, Bartolucci AA, Eberhardt AW. Nonlinear stress-strain behavior of periodontal ligament under orthodontic loading. *Am J Orthod Dentofacial Orthopedics* 2002;122:174-9.
37. Toms SR, Eberhardt AW. A nonlinear finite element analysis of the periodontal ligament under orthodontic tooth loading. *Am J Orthod Dentofacial Orthop* 2003;123:657-65.
38. von Bohl M, Kuijpers-Jagtman AM. Hyalinization during orthodontic tooth movement: a systematic review on tissue reactions. *Eur J Orthod* 2009;31:30-6.
39. Kim T, Suh J, Kim N, Lee M. Optimum conditions for parallel translation of maxillary anterior teeth under retraction force determined with the finite element method. *Am J Orthod Dentofacial Orthop* 2010;137:639-47.
40. Tominaga JY, Tanaka M, Koga Y, Gonzales C, Kobayashi M, Yoshida N. Optimal loading conditions for controlled movement of anterior teeth in sliding mechanics. *Angle Orthod* 2009;79:1102-7.
41. Sia S, Koga Y, Yoshida N. Determining the center of resistance of maxillary anterior teeth subjected to retraction forces in sliding mechanics. An in vivo study. *Angle Orthod* 2007;77:999-1003.
42. Jung MH, Kim TW. Biomechanical considerations in treatment with miniscrew anchorage. Part 1: the sagittal plane. *J Clin Orthod* 2008;42:79-83.
43. Brettin BT, Grosland NM, Qian F, Southard KA, Stuntz TD, Morgan TA, et al. Bicortical vs monocortical orthodontic skeletal anchorage. *Am J Orthod Dentofacial Orthop* 2008;134:625-35.

44. Viwattanatipa N, Thanakitcharu S, Utraravichien A, Pitiphat W. Survival analyses of surgical miniscrews as orthodontic anchorage. *Am J Orthod Dentofacial Orthop* 2009;136:29-36.
45. Kuroda S, Sugawara Y, Deguchi T, Kyung HM, Takano-Yamamoto T. Clinical use of miniscrew implants as orthodontic anchorage: success rates and postoperative discomfort. *Am J Orthod Dentofacial Orthop* 2007;131:9-15.
46. Sung SJ, Jang GW, Chun YS, Moon YS. Effective en-masse retraction design with orthodontic mini-implant anchorage: a finite element analysis. *Am J Orthod Dentofacial Orthop* 2010;137:648-57.